Accepted Manuscript

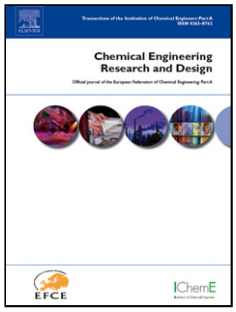

Title: Plasmonic Sensors in Multi-Analyte environment: rate constants and transient analysis

Author: Olga M. Jakšić Danijela V. Randjelović Zoran S. Jakšić Željko D. Čupić Ljiljana Z. Kolar−Anić

PII: S0263-8762(13)00280-3
DOI: http://dx.doi.org/doi:10.1016/j.cherd.2013.06.033
Reference: CHERD 1304

To appear in:

Received date: 25-3-2013
Revised date: 22-6-2013
Accepted date: 27-6-2013

Please cite this article as: Jakšić, O.M., Randjelović, D.V., Jakšić, Z.S., Čupić, Ž.D., Kolar−Anić, L.Z., Plasmonic Sensors in Multi-Analyte environment: rate constants and transient analysis, *Chemical Engineering Research and Design* (2013), http://dx.doi.org/10.1016/j.cherd.2013.06.033

Graphical Abstract (for review)

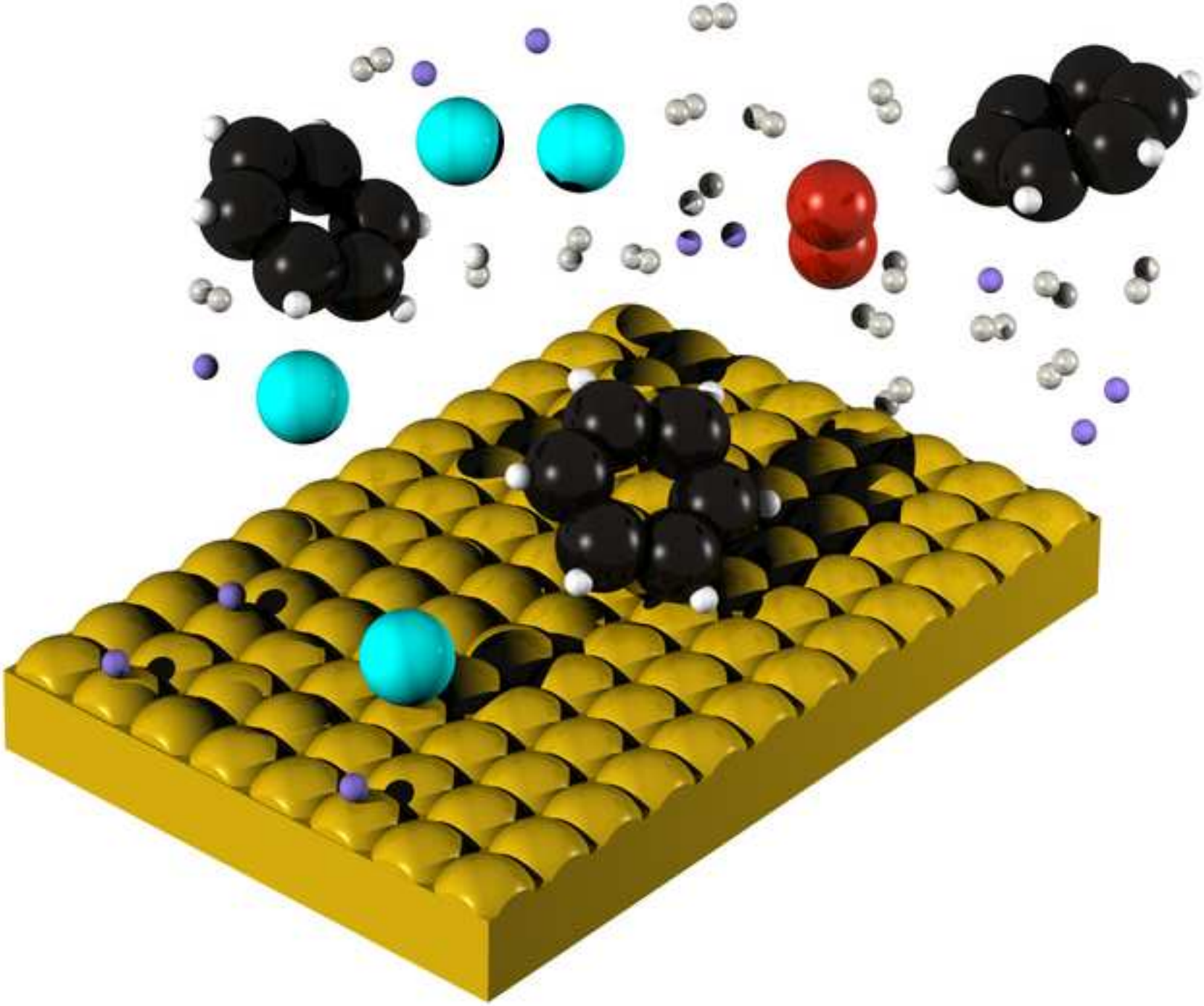

Plasmonic Sensors in Multi-Analyte environment: rate constants and transient analysis

Olga M. Jakšić[a], Danijela V. Randjelović[a], Zoran S. Jakšić[a], Željko D. Čupić[b] and Ljiljana Z. Kolar–Anić[c]

[a] *Centre of Microelectronic Technologies and Single Crystals, Institute of Chemistry, Technology and Metallurgy, University of Belgrade, Njegoševa 12, 11000 Belgrade, Serbia. e-mail: olga@nanosys.ihtm.bg.ac.rs*

[b] *Centre of Catalysis and Chemical Engineering, Institute of Chemistry, Technology and Metallurgy, University of Belgrade, Njegoševa 12, 11000 Belgrade, Serbia. e-mail: zcupic@nanosys.ihtm.bg.ac.rs*

[c] *Faculty of Physical Chemistry, University of Belgrade, Studentski trg 12-16, 11000 Belgrade, Serbia. e-mail: lkolar@ffh.bg.ac.rs*

corresponding author: Olga Jakšić,

corresponding author's institution: Centre of Microelectronic Technologies and Single Crystals, Institute of Chemistry, Technology and Metallurgy, University of Belgrade, Njegoševa 12, 11000 Belgrade, Serbia

Phone – (+) 381 11 2628 587

Fax - (+) 381 11 2182 995

e-mail olga@nanosys.ihtm.bg.ac.rs

ABSTRACT

This paper investigates multicomponent gas adsorption at the active surface of plasmonic chemical sensors and shows that there are situations where transients in a single sensor element can be used for simultaneous detection of different gases in multicomponent mixtures. A general master equation set is provided, describing multicomponent adsorption. Analytical expressions for sorption rates are derived and high-accuracy simplified models are proposed. Expressions for adsorption rate constants and rates and for number of binding sites are proposed. The derived analytical model takes into account the adsorbate molecule size, distribution of binding sites as determined by the crystallographic structure of the sensor surface and multi-site adsorption. The model allows for the calculation and optimization of deterministic behavior of the system. It is shown that trace amounts of target gas species can be made detectable by adding controlled amounts of known carrier gas. Besides being applicable in plasmonic sensor design and optimization, the obtained results may be of importance in situations where fast and low-cost detection of trace amounts of gases is needed, including natural gas leakage in residential heating, radon outgassing in dwellings, environmental protection, homeland defense and hazardous materials management, greenhouse footprint investigations, etc.

HIGHLIGHTS

- general equation set for multicomponent monolayer gas adsorption is derived
- analytical model of adsorption takes into account adsorbate molecule size
- adsorption rate constants are modeled using chemical software and data mining
- simultaneous plasmonic sensing of several gas species in mixture is considered

KEYWORDS:

Adsorption-desorption kinetics; Plasmonic sensor, Gas sensor, Multi-Analyte

1. INTRODUCTION

There is a need for simultaneous multi-analyte detection in various applications (gas chromatography, greenhouse gas footprint, etc.), but the available options are quite limited. Some of them are an early stage of investigation (Azcón et al., 2012; Basker & Zabe, 2012a, 2012b; Blecka et al., 2011; Lagrone et al., 2012; Macfie et al., 2012; Woudenberg et al., 2012) and some are constrained by the targeted number of analytes like in multi-channel sensor platforms for biosensing (Djurić et al., 2007; Homola et al., 2005; Yu & Li, 2009). Plasmonic sensors are especially promising as miniaturized optical devices fabricated by the use of nanostructures, nanoparticles and nano arrays (Stewart et al., 2008), having high sensitivities ($2.5 \cdot 10^{-8}$ for RI change, (Slavík & Homola, 2007)) and extremely fast read-out (according to (Byard et al., 2012), about a nanosecond). There are nanoengineered sensor platforms capable for the detection of two (Wright et al., 2012) or more analytes (Homola et al., 2005) simultaneously, but it is not always the case that the nanostructured array of sensors gives improvements over the single sensor area (Joy et al., 2012).

There is also another approach: single sensor employment. It has been investigated by monitoring the free diffusion-physisorption of the analytes in multiple microfluidic channels (Ghafarinia et al., 2012). Also, the surface of a single plasmonic sensor can be functionalized so that multiple modes of operation co-exist and enable simultaneous detection of different analytes (MacKay & Lakhtakia, 2012; Swiontek et al., 2013), but the fabrication of such a special surface, chiral sculptured thin film (CSTF), a form of biomimetic nanoengineered metamaterials, represents a significant technological challenge.

We address here the adsorption kinetics at the surface of a single-element plasmonic sensor and consider the possibility that the regular measurement with proper data analysis and interpretation might be sufficient for the multiple measurands identification.

Adsorption and desorption (ad) processes are crucial for the operation of micro and nano systems. They may be favorable like in adsorption-based bio and chemical sensors (Anker et al., 2008; Barnes et al., 2003; Eggins, 2002; Jaksic et al., 2009; Willets & Van Duyne, 2007), or they can be unfavorable, causing adsorption-induced mass fluctuations (Vig & Kim, 1999; Yong & Vig, 1989). Plasmonic sensors base their operation on the existence of a surface-bound electromagnetic wave at an interface between a medium with positive relative dielectric permittivity (air for instance) and another one with negative permittivity (good metals like gold or silver), coupled with collective oscillations of electron gas within the negative permittivity part. Alternative plasmonic materials (Boltasseva & Atwater, 2011) like e.g. transparent conductive oxides, intermetallic, graphene, etc. have also been studied, because they ensure lower absorption losses and wider choice of operating frequency ranges.

The established wave is denoted as the surface plasmon polariton (SPP). The adsorption of analyte particles at the interface causes the change of the dielectric permittivity in the location of field maximum that can be externally detected. There are two main classes of such sensors. One of them bases its principle of operation on propagating SPP (conventional surface plasmon resonance sensors), and the other on localized plasmons-polaritons (nanoparticle-based sensors) (Abdulhalim et al., 2008). All pplasmonic sensors ensure direct and label-free, real-time, all-optical detection of analytes with extreme sensitivities.

In addition to engaging the propagating and localized plasmon polaritons on the surface there is another degree of freedom in sensor design and it is ensured by nanostructuring plasmonic sensors, thus obtaining 1D, 2D or 3D subwavelength plasmonic crystals. Examples include nanoaperture or nanowire arrays and generally electromagnetic/optical metal-dielectric periodic metamaterials (Bingham et al., 2008; Kabashin et al., 2009).

In all of these cases even miniscule alterations of the surface refractive index greatly influence the device performance and it is of utmost importance to ensure maximum control and enable tailoring of adsorption-desorption processes with a goal to maximize sensor sensitivity and selectivity and at the same time to minimize intrinsic noise caused by adsorption-desorption fluctuations (Jaksic et al., 2009). Thus, there is an obvious interest to establish a connection between the fundamental parameters of the ad process with the particular data that can be measured, calculated or estimated with the satisfactory precision for a specific application. Adsorption-desorption kinetics for different combinations of adsorbate molecules and adsorbent surfaces has been studied in various applications. Till now, rich scientific heritage of gathered data exists in physico-chemical databases available in bookshelves searchable online, for instance Landolt-Börnstein series (http://www.springermaterials.com/docs/index.html) or Pubshem Substance and Compound online database (http://pubchem.ncbi.nlm.nih.gov/). But still, there are situations where literature data are unavailable and experimental gathering of new data is unacceptable for budget or safety reasons (toxic or hazardous materials), so the determination of adsorption kinetics of different agents on such materials remains a non-trivial problem. Most of the available literature dedicated to plasmonic sensors skips this

and goes directly for particular engineering solutions, while at the same time handling only a few materials (typically gold and silver for the plasmonic part) and defining specific methods and protocols for particular situations (De Mol & Fischer, 2010; Schasfoort & Tudos, 2008). This solves concrete engineering problems in a very satisfactory manner but at the same time hinders the possibility to optimize and enhance novel nanostructured sensors and impedes the introduction of new materials.

In this paper we derive a general analytical master equation set enabling modelling of multicomponent monolayer gas adsorption-desorption at different plasmonic sensor surfaces in various situations. We establish a connection between adsorption kinetics and material properties like the parameters of adsorbate gases including their atomic/molecular size as well as the crystallographic structure of the sensor surface. We present an estimation procedure to determine the number of adsorbed molecules for different material combinations in the case of multi-site adsorption. Finally we give some illustrative examples and their discussion.

2. THEORY AND CALCULATIONS

----------> Fig.1 <----------

We consider a situation schematically shown in Fig. 1 where the active solid sensor area A has a given surface density of binding sites n_s and is immersed in a finite container of a volume V, filled with a mixture of different gases, each at its partial pressure p_i and with its given molecular properties like molecular size, shape, orientation and mass. An adsorption site or binding site is defined as a

location at the adsorbent surface where the adsorbate can make a single bond; multi-site adsorption may occur if an adsorbate molecule is larger than a single binding site (Do, 1998). Our interest is to determine kinetics of simultaneous multicomponent monolayer adsorption of all of the different species present in the mixture. We assume that in the starting moment the adsorbent surface of the sensor is completely free, i.e. that its surface coverage by gas adsorbate molecules is zero.

Our initial assumptions are as follows: we consider a monolayer gas-solid surface adsorption-desorption process with one or more ideal gas species. All particles of the same gas species are interchangeable. Adsorbate particles do not collide or interact with each other (there is no dissociative adsorption). The surface is homogeneous (the active binding sites are equal) so that the average residential time of adsorbed particles is the same for all particles of the same gas species.

2.1 SINGLE SITE ADSORPTION

Although multi-site adsorption will be considered later in this text, it is more convenient to start from a situation when a single adsorbate molecule of any gas species in the mixture does not occupy more than one binding site. In this case, a multicomponent adsorption-desorption process can be modeled as a second order chemical reaction where $A_{g,i}$, a free gas molecule of the i_{th} gas species and a single free binding site, A_f, reversibly transforms into an adsorbed molecule of the i_{th} gas species, $A_{a,i}$, according to the following set of stoichiometric equations (Kolar-Anić et al., 2011)

$$A_{g,i} + A_f \underset{k_{ds,i}}{\overset{k_{as,i}}{\rightleftarrows}} A_{a,i} \ , \qquad (1)$$

where $k_{as,i}$ and $k_{ds,i}$ are the rate constants of the adsorption and desorption process of the i_{th} gas species in case of single site adsorption, respectively.

The time evolution of the number of adsorbed molecules for each gas species of the mixture in (1) is described by a differential equation from the following set:

$$\frac{dN_{a,i}}{dt} = k_{as,i} N_{g,i} N_f - k_{ds,i} N_{a,i}\,,\ i = 1,....,\ M\ . \qquad (2)$$

Here $N_{g,i}$ is the number of free gas molecules of the i_{th} gas species, $N_{a,i}$ is the number of adsorbed molecules of the i_{th} gas species and N_f is the number of free binding sites. The number of free binding sites is the same for all gas species. It is the number of free places available for adsorption at that moment. If the maximum number of free places, i.e. the overall number of binding sites on the active area is denoted as M, then, at any instance, gas molecules compete for the same number of free places on the same free surface and that number is

$$N_f = M - \sum_{j=1}^{r} N_{a,j}\ .$$

For each species there are two variables: the number of free non-adsorbed molecules and the number of the adsorbed ones. A molecule is either adsorbed on the surface or freely moving in the gas chamber. Since the gas mixture consists of r species, expression (2) represents a set of r equations, but keeping $N_{g,i}$ and $N_{a,i}$ both in one equation doubles the number of variables of interest. The system is closed, thus the overall number of molecules for each gas species $N_{0,i}$ remains constant during the observation time (from the initial moment when surface is without any adsorbate till the moment when the thermo-dynamical equilibrium is reached), such that the relation $N_{0,i} = N_{g,i} + N_{a,i}$ is always satisfied.

Since the initial partial pressure of a specific gas species is known, the overall number of molecules for each gas species, $N_{0,i}$, is also known.; equation set (2) becomes

$$\frac{dN_{a,i}}{dt} = k_{as,i}\left(N_{0,i} - N_{a,i}\right)\left(M - \sum_{j=1}^{r} N_{a,j}\right) - k_{ds,i}N_{a,i}\,. \qquad (3)$$

Equation set (3) describes a situation when a single adsorbate molecule of any gas species in the mixture does not occupy more than one binding site. A special case of that situation is mono-component adsorption (r = 1), described by Riccati equation that can be solved analytically (Kolar-Anić et al., 1985, 2011).

But in real situations some molecules can be large enough to cover several binding sites. In that case the number of molecules in a fully populated monomolecular mono-component layer is not the same for all gas species and the described model is no longer valid.

2.2 MULTI-SITE ADSORPTION

As seen in Fig. 1, the molecules of adsorbate (gas) cannot be packed closer than they are allowed by the layout and the size of the adsorbent atoms (top layer atoms at the plasmonic surface). On the other hand, large gas molecules may cover several binding sites when sticking to the surface, and in that case the number of free binding sites for other species and the number of molecules that can fully populate that surface in monolayer are not governed only by the adsorbent surface structure but also by the size of the adsorbate molecules.

When the mixture contains at least one gas species whose molecules need more than one binding site on the surface to be adsorbed (multi-site adsorption), then

the maximum number of adsorbed molecules on a completely free surface ceases to be equal to the number of binding sites M for that gas species. In order to make a distinction, let us denote with $M_{b,i}$ the maximum number of adsorbed molecules on a completely free surface *i.e*. the maximum number of binding places for the i_{th} gas species. That number depends on the molecular size and on the crystalographic structure of the surface and is calculated in different ways that depend on the ratio between the adsorbate molecule size, its geometry and the binding site area. For molecule sizes below that of a single binding site (Fig. 1a) or approximately equal to it (Fig. 1b), $M_{b,i}$ equals the number of binding sites, *i.e.* the number of binding sites M. For larger molecules whose adsorption involves more than a single binding site from the surface (Fig. 1c), $M_{b,i}$ is the maximal possible number of adsorbed molecules that can be calculated as the product of the surface density of adsorbed molecules and the active surface area. A problem with this approach is that the adsorbate surface density is a parameter rarely met in literature and different for various adsorbate-adsorbent combinations, so that it has to be experimentally determined for each material pair. An alternative approach is to estimate $M_{b,i}$ by the procedure outlined later in this text.

If we denote with S the active surface area of a sensor and with σ_i the surface density of adsorbed molecules for the gas species i, then the initial number of multi-site adsorption places on the given surface, available for adsorption of molecules of that gas species, will be

$$M_{b,i} = \sigma_i S . \quad (4)$$

It is the maximal number of places that a particular gas species can occupy in a fully populated monolayer on that surface. The instantaneous number of free

places on the surface for the gas species *i*, $N_{f,i}$, depends on the surface that is free at that moment, *i.e*. the difference between *S* and the sum of all the surface fractions occupied by adsorbed molecules of all gas species. At one instant, the total occupied surface equals the sum of all surfaces occupied by adsorbed molecules. Each gas species has its share on the surface (N_a/σ) and the instantaneous free surface can be approximated by the difference of *S* and the sum $\sum_{j=1}^{r} N_{a,j} \Big/ \sigma_j$. The instantaneous number of free places available for the adsorption of molecules of i_{th} gas species is then

$$N_{f,i} = \sigma_i \left(S - \sum_{j=1}^{r} \frac{N_{a,j}}{\sigma_j} \right) = M_{b,i} - \sigma_i \sum_{j=1}^{r} \frac{N_{a,j}}{\sigma_j} .$$

Actually, the connection between the free surface and the number of free places is not determined solely by the surface density of adsorbate molecules, since separate free adsorption centers do not form a free place for multisite adsorption unless they are grouped.

After the initial stage, an adsorbed molecule, $A_{a,i}$, reversibly transforms into a free gas molecule, $A_{g,i}$, and leaves a free multi-site adsorption place on the surface, $A_{b,i}$. If we employ new notation for this multisite adsorption case and denote with $k_{am,i}$ and $k_{dm,i}$ the rate constants of the multicomponent adsorption and desorption process of the i_{th} gas species, respectively, the modified stoichiometric equation applicable for this situation becomes

$$A_{g,i} + A_{b,i} \underset{k_{dm,i}}{\overset{k_{am,i}}{\rightleftharpoons}} A_{a,i} \ .$$

The corresponding differential equation, whose solution gives the time evolution of the adsorbed molecules of the i_{th} gas species, must be modified, since the effect of molecular size has been taken into account:

$$\frac{dN_{a,i}}{dt} = k_{am,i}\left(N_{0,i} - N_{a,i}\right)\left(M_{b,i} - \sigma_i \sum_{j=1}^{r} \frac{N_{a,j}}{\sigma_j}\right) - k_{dm,i} N_{a,i} . \quad (5)$$

In the above kinetic equations, the characteristics of gas-solid interactions in particular cases are included in the rate constants.

The focus of this work is on the question how the molecular size affects the rate constants.

2.3 RATE CONSTANT MODELING

In order to define rate constants necessary for gas sensing applications we use an approach based on the ideal gas theory. The overall dynamics of the adsorption-desorption process depends both on adsorption and desorption. The rate equation for the number of adsorbed molecules is obtained from the difference between the adsorption and the desorption rate. The adsorption rate is proportional to the incident molecular flux, to the free surface available for adsorption and to the proportion of the incident molecules that are adsorbed.

The flux $R_{a,i}$ of gas molecules of the species i arriving onto the solid surface is proportional to that species' partial pressure (Do, 1998), p_i

$$R_{a,i} = \frac{p_i}{\sqrt{2\pi m_i k_B T}} .$$

Here m_i is the mass of a single molecule of the i_{th} gas, k_B is the Boltzmann constant, and T is temperature.

In order to define the free surface area A_{free} we focus on the current fractions of occupied surfaces for each of the r surrounding gases, θ_j. These fractions depend on the number of adsorbed molecules and on the number of molecules of one gas in a fully populated monolayer on the surface θ_j

$$A_{free} = S\left(1 - \sum_{j=1}^{r} \theta_j\right) = S\left(1 - \sum_{j=1}^{r} \frac{N_{a,j}}{M_{b,j}}\right) \qquad j = 1,...,r\ .$$

For every particle that arrives at the active surface area A there is a certain probability that it will remain adsorbed. Let us denote that sticking probability with $\alpha_{s,i}$.

So, the final expression for the rate equation of the number of adsorbed molecules for i_{th} gas, obtained from the difference of adsorption rate and desorption rate, becomes

$$\frac{dN_{a,i}}{dt} = \frac{S\alpha_{s,i}}{\sqrt{2\pi m_i k_B T}} p_i \left(1 - \sum_{j=1}^{r} \frac{N_{a,j}}{M_{b,j}}\right) - \frac{N_{a,i}}{\tau_{r,i}}\ . \qquad (6)$$

Partial pressures depend on the number of gas molecules at any instant throughout the process. So the ideal gas equation holds at the beginning of the process when the surface is free and all molecules are in gaseous phase with $N_{0,i}$ gas molecules of the i_{th} gas, $p_{0,i}$ being its initial partial pressure and V being the gas chamber volume.

$$p_{0,i} V = N_{0,i} k_B T\ .$$

Later, when adsorption takes place, the same equation holds but some gas molecules are missing, $N_{g,i}$ is the number of molecules of the i_{th} species in gaseous phase, pressure drops to the instantaneous value of p_i. At any instant the sum of

adsorbed molecules and those in gas phase must be equal to the initial number of gas molecules, $N_{0,i}$. In order to make a correlation with (5) we transform (6) into

$$\frac{dN_{a,i}}{dt} = \frac{S\alpha_{s,i}}{V}\sqrt{\frac{k_B T}{2\pi m_i}}\left(N_{0,i} - N_{a,i}\right)\left(1 - \sum_{j=1}^{r}\frac{N_{a,j}}{M_{b,j}}\right) - \frac{N_{a,i}}{\tau_{r,i}}. \quad (7)$$

In situations where the surface density of adsorbed molecules of all gas species equals the surface density of binding sites on the surface, (7) is in agreement with the expression for single-site adsorption (3), which is repeated here for convenience:

$$\frac{dN_{a,i}}{dt} = \frac{S\alpha_{s,i}}{MV}\sqrt{\frac{k_B T}{2\pi m_i}}\left(N_{0,i} - N_{a,i}\right)\left(M - \sum_{j=1}^{r}N_{a,j}\right) - \frac{N_{a,i}}{\tau_r}. \quad (8)$$

Thus, the final expression for the gas adsorption rate constant in the case of multicomponent process where each molecule occupies only one site is described by a model that follows the pattern of *r* parallel second-order chemical reactions. In this case the following expression for the rate constant is valid

$$k_{as,i} = \frac{S\alpha_{s,i}}{MV}\sqrt{\frac{k_B T}{2\pi m_i}}, \quad (9)$$

while the desorption rate constant is

$$k_{ds,i} = \frac{1}{\tau_{r,i}}. \quad (10)$$

The analogy between (8) and (5) implies that in a general situation that includes multi-site adsorption, the final expression for the molecular size-dependent adsorption rate constant is

$$k_{am,i} = \frac{S\alpha_{s,i}}{M_{b,i}V}\sqrt{\frac{k_B T}{2\pi m_i}}. \quad (11)$$

The multi-site desorption rate constant is not affected by the molecular size, and is equal to the single-site desorption rate constant.

2.4 PHYSICAL PARAMETERS FOR ADSORPTION KINETICS

Using (9) and (10) for single-site processes or (10) and (11) for multi-site case one is able to define sorption rate constants as functions of measurable physical parameters of each gas species in the system (partial pressure, temperature, gas chamber volume, active surface area, mean residential time of adsorbed molecules). All controllable parameters can be used to tailor the adsorption process dynamics.

In some cases some parameters might be hard to obtain or interpret. Such is the desorption rate constant which has the same form for both models. It depends on the mean residential time of adsorbed molecules through their desorption energy $E_{d,i}$

$$\tau_{r,i} = \tau_{0,i} \exp\left({E_{d,i}}/{RT} \right), \qquad (12)$$

where τ_0 is the period of adatom vibrations perpendicular to the solid surface. It is assumed to be 10^{-13} s ($1/\nu$, where ν is the frequency of lattice thermal vibrations, $\approx 10^{13}$ Hz) (Venables, 2000).

Literature data for desorption energies is relatively scarce and usually defined for very specific gas-surface material pairs. Among the few sources of numerical data that can be used in the models described here are (Christmann, 2006; Wetterer et al., 1998). They refer to the adsorption of hydrocarbons on gold. Data on

adsorption of molecules on metallic, semiconductor and oxide surfaces can be found in Landolt Bornstein handbooks.

Next we rewrite the expressions for the adsorption rate constant in terms of the surface density of binding sites (free spaces in the case of multi-site adsorption), rather than using their number. The multi-site adsorption rate constant (12) can be rewritten using (4) as

$$k_{am,i} = \frac{\alpha_{s,i}}{\sigma_i V}\sqrt{\frac{k_B T}{2\pi m_i}}\,.$$

On the other hand, in the expression for the rate constant for the adsorption in case of single-site adsorption surface the density of adsorbate molecules for all gas species that follow the single-site adsorption pattern equals the surface density of adsorption centers on the surface of the adsorbent material used for sensor fabrication.

$$k_{as,i} = \frac{\alpha_{s,i}}{\sigma V}\sqrt{\frac{k_B T}{2\pi m_i}}\,.$$

To our best knowledge, there are no available systematic databases for the surface density of adsorbed molecules or the surface density of binding sites, and obtaining these data from experimental sets for each particular case could be both complex and time consuming. Because of this we propose here a simple general procedure to obtain their approximate values.

For single-site adsorption the surface density of adsorbate may be straightforwardly estimated if the crystallographic structure of the adsorbent is known.

Molecules with their projected area smaller than the area of a binding site cannot be packed denser than allowed by the binding sites, which is determined by the

crystalographic structure of the adsorbent material. Thus the feasible surface density of adsorbed molecules is the minimum between the fictive calculated surface density of adsorbate molecules which disregards the surface structure and the real surface density of adsorbent molecules on the top layer. Typical materials for plasmonic sensors are good metals like silver, gold, copper. All of these have a face-centered cubic lattice (FCC). For instance, it is observed from the density calculated from the molar mass of gold (196.97 g) and from its unit cell size (0.40786 nm) that the distance between the binding sites of gold may be either 0.40786 nm or 0.2884 nm, hence the density of binding sites for gold, n_s, might be about 4 molecules/nm^2. This estimated value is very close to the data Leung reported in (Leung, 2005), where it is said: "A flat metal surface typically has a surface binding site density 10^{-5} moles/m^2 or $6{\cdot}10^{18}$ sites/m^2".

For the case of multi-site adsorption the task of determining the adsorbate surface density σ_i is different. One of the problems here is that non-spherical molecules of the same gas species can occupy different areas depending on their orientation with respect to the adsorbent surface (Gopal & Lee, 2006). For non-spherical molecules there are preferable orientations for physisorption and chemisorption so that in modeling one could treat all molecules of the same gas species in the same manner. An additional problem is that the available experimental data on surface density of adsorbate most often refer to the equilibrium case and are thus not usable for calculating the adsorption rate constants. The use of computational procedures such as *ab initio* calculus or the method based on extended Hückel molecular orbital theory may ease interpreting scanning tunneling microscope images, predict surface features of given adsorbate, their preferred binding sites

and orientations (Futaba & Chiang, 1999) but it may also be cumbersome and time consuming.

Our procedure for obtaining a quick estimate of the surface density of adsorbed molecules is based on the use of chemical software and data mining. First, the molecule structure is obtained using the chemical structure information available in the PubChem Substance and Compound online database through the unique chemical structure identifier CID (National Centre for Biotechnology Information. PubChem Substance and Compound database 2012). The molecular projected area can be then obtained using the program Marvin 5.9.3, 2012, ChemAxon (ChemAxon, 2012). The obtained results are further modified with an appropriate correction factor. The spheres do not cover rectangular areas completely, so in order to take that into account, the molecular projected areas should be corrected by a factor of $4/\pi$. The fact that separate free adsorption centres on the surface do not form a free multisite adsorption place unless they are grouped, can be argued from a probabilistic point of view and an additional correction factor can be set, related to the probability that there are classes of grouped adjacent sites among N_f free adsorption centres. A different value of the additional correction factor may be used in case there are unusable fractions of the free surface (e.g. if the surface is nanostructured like in the case of subwavelength plasmonic crystal or metamaterial-based sensors (Anker et al., 2008)) or the adsorbent topology affects the surface density of adsorbed molecules for some other reason. Finally the reciprocal value of the projected area is used to obtain the maximal number of free places available for adsorption per unit area for different gas species.

Numerical data for the rate constants are necessary for the further qualitative and quantitative study, i.e. for the analysis of transients and equilibrium states by

using the phenomenological kinetic approach. The molecular projected area, needed for the calculation of the surface density of adsorbed molecules and the calculation of the number of binding sites on the surface, was determined in the above described manner and the obtained data were compared with the available literature data. For instance, the surface densities of adsorbed molecules, given in 10^{18} molecules/m^2 would be 7.7 for oxygen, 6.6 for nitrogen, 6.1 for carbon dioxide, 6.6 for carbon monoxide and 6.3 for methane, according to the experimental results from (Do, 1998). For the same gases our estimation procedure gives relatively close values: 7.34 for oxygen, 7.5 for nitrogen, 6.52 for carbon dioxide, 7.15 for carbon monoxide and 6.52 for methane. A similar degree of accuracy is obtained for other gases. A comparison of the surface density of adsorbed molecules determined utilizing the calculated molecular projected areas with the data given by Gland (Gland, 1980) also give a good agreement. Thus we consider our approach suitable for preliminary investigations of the adsorption of arbitrary gases (industrial pollutants, hazardous, military chemical agents like nerve gases and vesicants, etc.).

3. METHOD

Using the approach presented in this work it is possible, in gas sensing for instance, to explore the time evolution and hence the temporal response which indicates the speed of operation, transient response which gives insight into any overshoots that might occur before the sensor reaches its steady-state response, but also into the steady-state itself, as well as the minimum detectable signal, noise, device sensitivity and selectivity.

One can calculate the time evolution of the number of adsorbed molecules by solving the master equation set (3) or (5). These equation sets are Riccati type matrix differential equations. We demonstrate here the application of our results for the case of a single-component gas mixture. The solution of (3) in the single-site single-component case is (Kolar-Anić et al., 1985, 2011):

$$N_{a,1(3)}(t) = \frac{\gamma_{(3)}\beta_{(3)}\left[1-\exp\left(-k_{as,1}\left(\gamma_{(3)}-\beta_{(3)}\right)t\right)\right]}{\gamma_{(3)}-\beta_{(3)}\exp\left(-k_{as,1}\left(\gamma_{(3)}-\beta_{(3)}\right)t\right)},$$

where

$$\gamma_{(3)} = \frac{1}{2}\left[\frac{k_{ds,1}}{k_{as,1}} + N_0 + M + \sqrt{\left(\frac{k_{ds,1}}{k_{as,1}} + N_0 + M\right)^2 - 4N_0M}\right],$$

$$\beta_{(3)} = \frac{1}{2}\left[\frac{k_{ds,1}}{k_{as,1}} + N_0 + M - \sqrt{\left(\frac{k_{ds,1}}{k_{as,1}} + N_0 + M\right)^2 - 4N_0M}\right].$$

The single-component case for multisite adsorption, the solution of (5), has the same form safe for the use of different rate constants and the different maximums of available adsorption places M_b.

The solution to a system of r interdependent Ricatti equations is more suitable for numerical procedures than analytical, but in most practical situations approximation can be made. In (Arakelyan et al., 2008) it is shown that if the equilibrium constant (the ratio of adsorption rate constant and desorption rate constant) is small or the number of adsorbed molecules is smaller than that in the gas phase, adsorption-desorption process may be treated as isobaric (at any instant the number of adsorbed molecules is so small that the initial pressure does not

drop). For the number of adsorption places in micro and nanostructures (the maximum possible number of adsorbed molecules) that condition is satisfied. In that case, equations in sets (3) or (5) become linear differential equations:

$$\frac{dN_{a,i}}{dt} = k_{ls,i}\left(M - \sum_{j=1}^{r} N_{a,j}\right) - k_{ds,i}N_{a,i}$$

$$\frac{dN_{a,i}}{dt} = k_{lm,i}\left(M_{b,i} - \sigma_i \sum_{j=1}^{r} \frac{N_{a,j}}{\sigma_j}\right) - k_{dm,i}N_{a,i}\,.$$

The rate constants for desorption can be calculated using (10) and the new rate constants for adsorption in the cases of multi-site and single-site adsorption are

$$k_{lm,i} = \frac{\alpha_{si}\, p_i S}{M_{b,i}\sqrt{2\pi m_i k_B T}} \qquad k_{ls,i} = \frac{\alpha_{si}\, p_i S}{M\sqrt{2\pi m_i k_B T}}\,. \qquad (13)$$

Under these circumstances, the solution to the single component case of (3) is

$$N_a(t) = \frac{Mk_l\left(1 - e^{-(k_l + k_d)t}\right)}{k_l + k_d}\,, \quad (14)$$

and the solution to multi-component case can be obtained in analytical form using the Laplace transform.

A more realistic situation is met if there are residual adsorbed gases at the substrate prior the beginning of the observed process. For real samples there is always exposure of the plasmonic surface to some kind of background gases, for instance to the air. Thus we need to extend our consideration to the case when the initial condition is non-zero and the time evolution starts from some finite value. Equations (3)-(8) that constitute our model are general and can be used both in the case of zero and of non-zero background, while residual adsorption can be

arbitrary. Background exposure is modeled by additional component/components in the mixture and the pre-existence of any component is modeled by different initial condition in differential equations, as stated before.

Further we consider single-component adsorption with non-zero background. To this purpose we assume that the pressure in the system before the moment $t = 0$, was not zero but p^*. By using p^* instead of p equation (6), and by putting the left hand side of (6) to zero and solving it, one gets the value $N_a(0)$ that refers to the previously established equilibrium. We use $N_a(0)$ as new initial condition instead of zero. The solution (14) is now

$$N_a(t) = \frac{Mk_l}{k_l + k_d} + \left[N_a(0) - \frac{Mk_l}{k_l + k_d} \right] e^{-(k_l + k_d)t}.$$

The identical approach is used for the multi-component case.

Further we consider the sensor output. The number of adsorbed molecules cannot be measured directly. A plasmonic sensor senses the refractive index change instead. To establish the connection between the refractive index change and the number of adsorbed molecules, the standard approach for the determination of optical coefficients for layered thin films for TM polarization of surface electromagnetic waves (Cai & Shalaev, 2010) can be used, so the effective value of refractive index change is calculated by the use of the method of weighted averages (Jakšić et al., 2010)

$$n_{eff} = wN_a = \frac{n_a - n_e}{M} N_a, \qquad (15)$$

where w equals the difference between the refractive index of the adsorbate n_a and the refractive index of the environment n_e, normalized with the maximum possible

number of adsorbed molecules (M or M_b depending if the situation is with single site adsorption or multisite adsorption).

Analogously, in multicomponent case where molecules of r different gas species compete for an adsorption place on the same sensor surface the effective value of refractive index change is calculated by

$$n_{eff} = \sum_{i=1}^{r} w_i N_{a,i} = \sum_{i=1}^{r} \frac{n_{a,i} - n_e}{M} N_{a,i} .$$

4. RESULTS

----------> Fig.2 <----------

Figure 2 shows the time evolution of the number of adsorbed molecules in case of single-component adsorption for five different situations occurring in practice (hexane and oxygen adsorption on gold, hydrogen adsorption on nickel and adsorption of carbon dioxide on iron and palladium). Numerical data for desorption energies were adopted from (Christmann, 2006; Fichthorn & Miron, 2002; Wetterer et al., 1998). All calculations were done for room temperature, a volume of 3 lit, a pressure of 0.05 Pa and a surface area of 1 cm^2. For the same initial number of gas molecules and the same adsorbent/sensor surface area of 1 cm^2 different transient times and equilibrium values are obtained. That difference is a consequence of the effect of the molecular size and weight and can be used in qualitative and quantitative analysis if analyte is unknown. We see also that gas adsorption is a fast process and that, at room temperature, typical plasmonic sensor would record equilibrium values.

----------> Fig.3 <----------

Figure 3 shows time evolution of refractive index for different pressures and temperatures in case of hexane detection with plasmonic sensor surface of gold. Typical response has a knee between a flat plateau indicating the equilibrium and a constant slope rise defining rise time or response time of a sensor. At lower pressures and lower temperatures the knee is detectable since the state-of-the-art plasmonic sensors are fast enough (Byard et al., 2012).

If we want to deduce the measured gas properties (in case of field applications where the measurand is known) based on a single regular measurement with a plasmonic sensor, without the expensive/massive laboratory equipment, we must then find a correlation between one set of data comprising the knee position and plateau level and another set that includes the rate constants and the weighted factor *w*. In case of a single component gas, for practical situations where (14) and (15) hold, the task is equivalent to finding a known-function-three-parameter-fit for measured data. If we ensure that the knee is detectable (by controlling the environmental conditions: lowering pressure and temperature) after obtaining the rate constants and *w*, we then go backwards through equations presented in this paper and calculate desorption energy, refractive index, etc.

----------> Fig.4 <----------

Figure 4 shows multicomponent adsorption where molecules of 3 gases, whose molecular weights and desorption energies are close to each other (Wetterer et al., 1998), compete for the same number of adsorption places on a sensor surface of gold. Figure 4 indicates that, unless we are certain about the number of components in gas mixture, fitting may be deceiving, for there is no noticeable change of slope and only one knee appears. Two sets of curves are given, one corresponding to the temperature of 200 K (printed in blue) and the other

corresponding to the temperature of 250 K (printed in red). Each of them comprises the refractive index change due to the presence of the three component mixture (solid line with stars), curves of the refractive index change for each separate component (dotted or diamonds for hexane, dashed or squares for heptane and dash dotted or circles for benzene), and curves for the refractive index change due to the adsorption of every separate gas as if it were alone (blue or red solid lines). This figure is important for it reveals that the presence of additional gases in mixture does not remarkably influence the time that a single gas takes to reach the equilibrium on its own. However, it affects the equilibrium value. Even small amounts of gas added to a mixture (the heptane pressure is three orders of magnitude lower of that of hexane and benzene), lead to lowering the equilibrium value of refractive index for the adsorbed gas (compared to the equilibrium value for single gas adsorption). This effect is here demonstrated by blue curves corresponding to the temperature of 200 K. Red curves, that correspond to the temperature of 250 K, demonstrate that there are situations where gases don't influence one another: the refractive index change due to the adsorption of every separate gas as if it were alone (solid lines) coincides with the calculated contribution of each separate component to the refractive index change (symbols). That means that instead of solving *r* second order Riccati equations numerically, or *r* linear differential interdependent equations analytically, one may simply add contributions of separate gases treated separately and make a quick rough estimate about the sensor response.

The degree of the mutual influence of gases in multicomponent mixtures will obviously depend on the parameters of the particular gases in the mixture. A low influence will be observed if gases are relatively similar – for instance, the

molecular weights and the desorption energies of gases are close to each other. However, if gases are reactive or significantly more (or less) "aggressive" toward the adsorbent, the situation will be completely different and the mutual influence will not be negligible.

----------> Fig.5 <----------

Figure 5 shows the situation where the existence of two "knees" in the transient response indicates the presence of at least two gases in the mixture. The mixture contains methane at a partial pressure of 0.9 mPa, CO_2 at a partial pressure of 0.3 mPa and traces of benzene (its partial pressure is 1 μPa) at 200 K. The individual contribution of methane is beyond the detection limit, but that makes the problem easier to analyze. Compared to carbon-dioxide or higher hydrocarbons, methane has low desorption energy (Koel et al., 2006; Wetterer et al., 1998), it reaches very fast the equilibrium and the existence of any knee (for that combination of pressure/temperature) indicates the presence of impurities from natural gas, landfill gas or biogas. Based on Fig. 5 one may also conclude the nature of that gas (natural gas does not contain carbon-dioxide, biogas has up to 40% of it and landfill gas has up to 50%). Figure 5 is also representative for situations where trace amounts of gases can be made detectable by adding large amounts of known carrier gas: if we cannot detect traces of a gas alone (here it is benzene), we add large quantity of another gas (or gases) and the presence of otherwise undetectable gas is revealed (here, the highest knee corresponds to benzene).

----------> Fig.6 <----------

The transient response presented in Fig. 6 shows an important case when the gas background is non-zero and there is a significant amount of pre-adsorbed gas particles at the plasmonic surface. We analyzed a situation when there is a

background of nitrogen at near-atmospheric pressure to which a pollutant gas (benzene or sulfur dioxide) is added at the initial moment in an amount much smaller than the background (up to 100,000 times smaller). Since there is an initial value of the refractive index of the adsorbed analyte, the addition of a pollutant causes a change of the readout that we denote by Δn_{eff}. The calculation has been done for a gold substrate temperature of 250 K. The relative refractive index changes at the adsorbent surface are sufficiently high to be detected by the state-of-the art plasmonic sensors.

Recording transient response of plasmonic sensor gives insight into sorption dynamics and sorption rate constants of measured gases. Rate constants are related to known gas parameters (size, mass, refractive index) that are collected in available chemical databases or obtainable by the use of chemical software. They are also related to the gas parameters that are not so easy to estimate, like desorption energy. That means that by recording the transient response of a plasmonic sensor one may recognize or rule out the presence of specific gases in certain situations but it means also that by recording transient response of a plasmonic sensor one may deduce unknown gas properties from the estimated rate constants.

According to (10), desorption rate constant does not depend on the molecular size but rather on the interaction between the adsorbate molecules and the binding sites on the surface as governed by the desorption energy. The only system parameter that affects the desorption rate is temperature. Increasing temperature causes rise of the desorption rate constant. Measuring transient response at different temperatures gives insight into desorption energy.

5. CONCLUSIONS

The kinetics of adsorption at a plasmonic sensor surface is modelled for an arbitrary multicomponent gas mixture and analytical expressions are derived for all addressed situations. A method for the estimation of the surface density of binding sites for arbitrary gas species is proposed, taking into account binding site distribution, adsorbate molecular size and multi-site adsorption.

It is demonstrated how the rate constants derived here enable quantification of important figures of merit in the phenomenological kinetic analysis and the analysis of both transient and equilibrium states, as well as the stochastic analysis.

The presented results show that simultaneous sensing of multiple analytes using a single-element plasmonic sensor may be possible with proper device calibration and transient response data analysis. Consequently, sensor dimensions could be reduced compared to the state of the art devices. It is also shown that in some situations measurement of adsorption transients in multi-species environment may improve sensing of trace amounts of gases by adding controlled amounts of other gases, thus ensuring detection of species that would else be below the detection threshold.

The results represent a tool that could be useful in further research in the fields of adsorption and plasmonics. Besides being useful for fundamental investigations of gas/solid interactions and gas properties, the present analysis is applicable in various practical situations where early detection of gas leakage and sensing of trace amounts of gases is required in general. These range from the natural gas leakage in residential systems and industrial burners, carbon monoxide presence in automotive applications, radon outgassing from the walls in homes, presence of

trace amounts of chemical agents and explosive vapours in homeland defence, early warning to toxic spillage in environmental protection and hazardous material management, to such applications as early warning to volcanic and limnic eruptions based on released fumes, spacecraft appliance outgassing and many more.

ACKNOWLEDGEMENTS

This work was funded by Serbian Ministry of Education, Science and Technological Development through the projects TR 32008, III 45001, and ON 172015.

REFERENCES

Abdulhalim, I., Zourob, M., & Lakhtakia, A. (2008). Surface Plasmon Resonance for Biosensing: A Mini-Review. Electromagnetics, 28(3), 214–242.

Anker, J. N., Hall, W. P., Lyandres, O., Shah, N. C., Zhao, J., & Van Duyne, R. P. (2008). Biosensing with plasmonic nanosensors. Nat. Mater., 7(6), 442–453.

Arakelyan, V. B., Mamasakhlisov, E. S., Morozov, V. F., Navoyan, Z. E., & Arakelyan, a. V. (2008). Stochastic model of adsorption of particles on macromolecules at an arbitrary filling. Journal of Contemporary Physics (Armenian Academy of Sciences), 43(1), 48–52.

Azcón, J. R., Baeza, F. J. S., Colas, M. P. M., Nikiforov, A. B., Abramova, N., & Ipatov, A. (2012). Multi-analyte system and method based on impedimetric measurements. patent No. EP2515103A1.

Barnes, W. L., Dereux, A., & Ebbesen, T. W. (2003). Surface plasmon subwavelength optics. *Nature*, *424*(6950), 824–830.

Basker, C. J., & Zabe, N. A. (2012a). Multi-analyte affinity column for analyzing aflatoxin, fumonisin, ochratoxin and zearalenone. patent No. EP1787698B1

Basker, C. J., & Zabe, N. A. (2012b). Multi-analyte affinity column for analyzing aflatoxin, ochratoxin , zearalenone and deoxynivalenol. patent No. US20070117219.

Bingham, C. M., Tao, H., Liu, X., Averitt, R. D., Zhang, X., & Padilla, W. J. (2008). Planar wallpaper group metamaterials for novel terahertz applications. Optics Express, 16(23), 18565–18575.

Blecka, L., Seamer, L., Rastogi, S., Tsai, C., Jafari, N., & Lafredo, K. J. (2011). System and method for multi-analyte detection. patent No. US7955555.

Boltasseva, A., & Atwater, H. A. (2011). Low-loss plasmonic metamaterials. Science, 331(6015), 290–291.

Byard, C. L., Han, X., & Mendes, S. B. (2012). Angle-multiplexed waveguide resonance of high sensitivity and its application to nanosecond dynamics of molecular assemblies. Anal. Chem., 84(22), 9762–7.

Cai, W., & Shalaev, V. M. (2010). Optical Metamaterials: Fundamentals and Applications. Springer New York.

ChemAxon. (2012). Chemical software development platforms and desktop applications for the biotechnology and pharmaceutical industries. http://www.chemaxon.com

Christmann, K. (2006). 3.4.1 Adsorbate properties of hydrogen on solid surfaces. In H. P. Bonzel (Ed.), Adsorbed Layers on Surfaces. Part 5: Adsorption of molecules on metal, semiconductor and oxide surfaces (Vol. 42A5, pp. 1–130). Springer Berlin Heidelberg.

De Mol, N. J., & Fischer, M. J. E. (2010). Surface Plasmon Resonance: Methods and Protocols, Springer-Verlag New York.

Djurić, Z., Jokić, I., Frantlović, M., & Jakšić, O. (2007). Fluctuations of the number of particles and mass adsorbed on the sensor surface surrounded by a mixture of an arbitrary number of gases. Sens. Actuators, B, 127(2), 625–631.

Do, D. D. (1998). Adsorption Analysis: Equilibria and Kinetics (Vol. 2). Imperial College Press. London

Eggins, B. R. (2002). Chemical Sensors and Biosensors. Wiley.

Fichthorn, K., & Miron, R. (2002). Thermal Desorption of Large Molecules from Solid Surfaces. Phys. Rev. Lett., 89(19).

Futaba, D. N., & Chiang, S. (1999). Calculations of Scanning Tunneling Microscopic Images of Benzene on Pt (111) and Pd (111), and Thiophene on Pd (111). Jpn. J. Appl. Phys., 38(6), 3809–3812.

Ghafarinia, V., Amini, A., & Paknahad, M. (2012). Gas identification by a single gas sensor equipped with microfluidic channels. Sensor Letters, 10(3-4), 845–849.

Gland, J. L. (1980). Molecular and atomic adsorption of oxygen on the Pt(111) and Pt(S)-12(111) × (111) surfaces. Surf. Sci., 93(2-3), 487–514.

Gopal, A., & Lee, K. Y. C. (2006). Headgroup percolation and collapse of condensed langmuir monolayers. J. Phys. Chem, B, 110(44), 22079–87.

Homola, J., Vaisocherová, H., Dostálek, J., & Piliarik, M. (2005). Multi-analyte surface plasmon resonance biosensing. Methods, 37, 26–36.

Jaksic, Z., Jakšić, O., & Matović, J. (2009). Performance limits to the operation of nanoplasmonic chemical sensors: noise-equivalent refractive index and detectivity. J. Nanophotonics, 3(1), 031770.

Jakšić, O., Jakšić, Z., & Matović, J. (2010). Adsorption–desorption noise in plasmonic chemical/biological sensors for multiple analyte environment. Microsystem Technologies, 16(5), 735–743.

Joy, N. a, Rogers, P. H., Nandasiri, M. I., Thevuthasan, S., & Carpenter, M. a. (2012). Plasmonic-based sensing using an array of Au-metal oxide thin films. Anal. Chem., 84(23), 10437–44.

Kabashin, A. V, Evans, P., Pastkovsky, S., Hendren, W., Wurtz, G. A., Atkinson, R., … Zayats, A. V. (2009). Plasmonic nanorod metamaterials for biosensing. Nat. Mater., 8(11), 867–871.

Koel, B. E., Panja, C., Kim, J., & Samano, E. (2006). 3.8.4 CO2, NO2, SO2, OCS, N2O, O3 on metal surfaces. In H. P. Bonzel (Ed.), Adsorbed Layers on Surfaces. Part 5: Adsorption of molecules on metal, semiconductor and oxide surfaces (Vol. 42A5, pp. 1–72). Springer Berlin Heidelberg.

Kolar-Anić, L., Cvjetićanin, N., & Nikolis, G. (1985). The stochastic approach to monolayer adsorption: Fluctuations in the adsorbed amount. J. Serb. Chem. Soc., 50, 483–491.

Kolar-Anić, L., Čupić, Ž., Vukojević, V., & Anić, S. (2011). The dynamics of nonlinear processes. Belgrade: Faculty of Physical Chemistry.

Lagrone, M., Leuschen, M., O'Dell, D. B., & Zacharias, K. (2012). Multi-analyte detection system and method. patent No.EP2513626A2

Leung, M. (2005). Surface contamination from radon progeny. In AIP Conference Proceedings (Vol. 785, pp. 184–190).

Macfie, G., Webster, G., Cardosi, M. F., Leach, C. P., Setford, S., & Saini, S. (2012). Dual chamber, multi-analyte test strip with opposing electrodes. patent No. US8323467B2

MacKay, T. G., & Lakhtakia, A. (2012). Modeling chiral sculptured thin films as platforms for surface-plasmonic- polaritonic optical sensing. IEEE Sens. J., 12(2), 273–280.

Schasfoort, R. B. M., & Tudos, A. J. (2008). Handbook Of Surface Plasmon Resonance. (R. B. M. Schasfoort & A. J. Tudos, Eds.), RSC Pub Cambridge, London.

Slavík, R., & Homola, J. (2007). Ultrahigh resolution long range surface plasmon-based sensor. Sens. Actuators, B, 123(1), 10–12.

Stewart, M. E., Anderton, C. R., Thompson, L. B., Maria, J., Gray, S. K., Rogers, J. a, & Nuzzo, R. G. (2008). Nanostructured plasmonic sensors. Chem. Rev., 108(2), 494–521.

Swiontek, S. E., Pulsifer, D. P., & Lakhtakia, A. (2013). Optical sensing of analytes in aqueous solutions with a multiple surface-plasmon-polariton-wave platform. Sci. Rep., 3.

Venables, J. A. (2000). Introduction to Surface and Thin Film Processes. Cambridge University Press, London.

Vig, J. R., & Kim, Y. (1999). Noise in microelectromechanical system resonators. IEEE Trans Ultrason Ferroelectr Freq Control, 46(6), 1558–1565.

Wetterer, S. M., Lavrich, D. J., Cummings, T., Bernasek, S. L., & Scoles, G. (1998). Energetics and Kinetics of the Physisorption of Hydrocarbons on Au(111). J Phys Chem B, 102(46), 9266–9275.

Willets, K. A., & Van Duyne, R. P. (2007). Localized surface plasmon resonance spectroscopy and sensing. Annu. Rev. Phys. Chem., 58, 267–297.

Woudenberg, T., Albin, Michael (Antioch, C., Kowallis, Reid B. (Burlingame, C., Raysberg, Yefim (Fremont, C., Ragusa, Robert P. (Los Altos, C., & Winn-Deen, Emily S. (Potomac, M. (2012). Device and method for multiple analyte detection. patent No. 8119423

Wright, J. B., Cicotte, K. N., Subramania, G. C., Dirk, S. M., & Brener, I. A. (2012). Chemoselective gas sensors based on plasmonic nanohole arrays. Opt. Mater. Express, 2(11), 1655–1662.

Yong, Y. K., & Vig, J. R. (1989). Resonator Surface Contamination - A Cause of Frequency fluctuations? IEEE Trans Ultrason Ferroelectr Freq Control, 36(4), 452–458.

Yu, H., & Li, X. (2009). Bianalyte mass detection with a single resonant microcantilever. Appl. Phys. Lett., 94(1), 011901.

FIGURE CAPTIONS

Figure 1 Schematic representation of the homogeneous surface of an adsorbent surrounded by a mixture of different gases. White dashed outline defines a single binding site. Three cases of physisorption of different species are shown: a) helium atom (monatomic gas, size smaller than the binding site dimensions); b) argon atom (here comparable to the binding site size); c) benzene molecule (much larger than the binding site)

Figure 2 Time evolution of the number of adsorbed molecules in case of single-component adsorption for six different realistic situations. Black dashed line: hexane on gold, dotted magenta line: oxygen on gold, cyan solid line: hydrogen on nickel, red dash dotted line: carbon dioxide on iron; black solid line with symbol |: carbon dioxide on palladium

Figure 3 Time evolution of the refractive index due to hexane adsorption on gold for different pressures and temperatures. Dashed lines correspond to pressure of 1Pa and solid lines correspond to pressure of 1 μPa. Thin blue lines correspond to temperature of 200 K, thicker green lines correspond to temperature of 300 K and thickest red lines correspond to temperature of 400 K

Figure 4 Time evolution of the refractive index due to adsorption of 3 gas mixture (hexane and benzene at 1 μPa, heptane at 5 pPa) on plasmonic sensor active surface of gold for different pressures and temperatures, represented with a red solid line. Dashed line corresponds to calculated component due to hexane contribution, dashed line corresponds to calculated component due to heptane contribution, and dash-dot line corresponds to calculated component due to benzene contribution. Next to each component, blue solid line corresponds to the refractive index change due to the presence of that particular gas alone on its unchanged partial pressure and at the same temperature of 200 K

Figure 5 Time evolution of the refractive index due to adsorption of three-gas mixture (methane at partial pressure of 0.9 mPa, carbon-dioxide at partial pressure of 0.3 mPa and benzene at partial

pressure of 700 nPa) on gold at a temperature of 250 K (Red solid line.) Calculated contribution of methane corresponds to dotted black line, blue dash-dot is used for benzene and green dashed for carbon-dioxide.

Figure 6 Time evolution of the refractive index change due to adsorption of gases in case of non-zero background. Benzene (solid lines, blue) or sulfur dioxide (dashed lines, red) are added in the initial moment $t = 0$ to a nitrogen atmosphere. N_2 partial pressure is 90 kPa, while C_6H_6 partial pressures are (0.1 – 100) Pa, and SO_2 pressures are 1 Pa and 100 Pa.

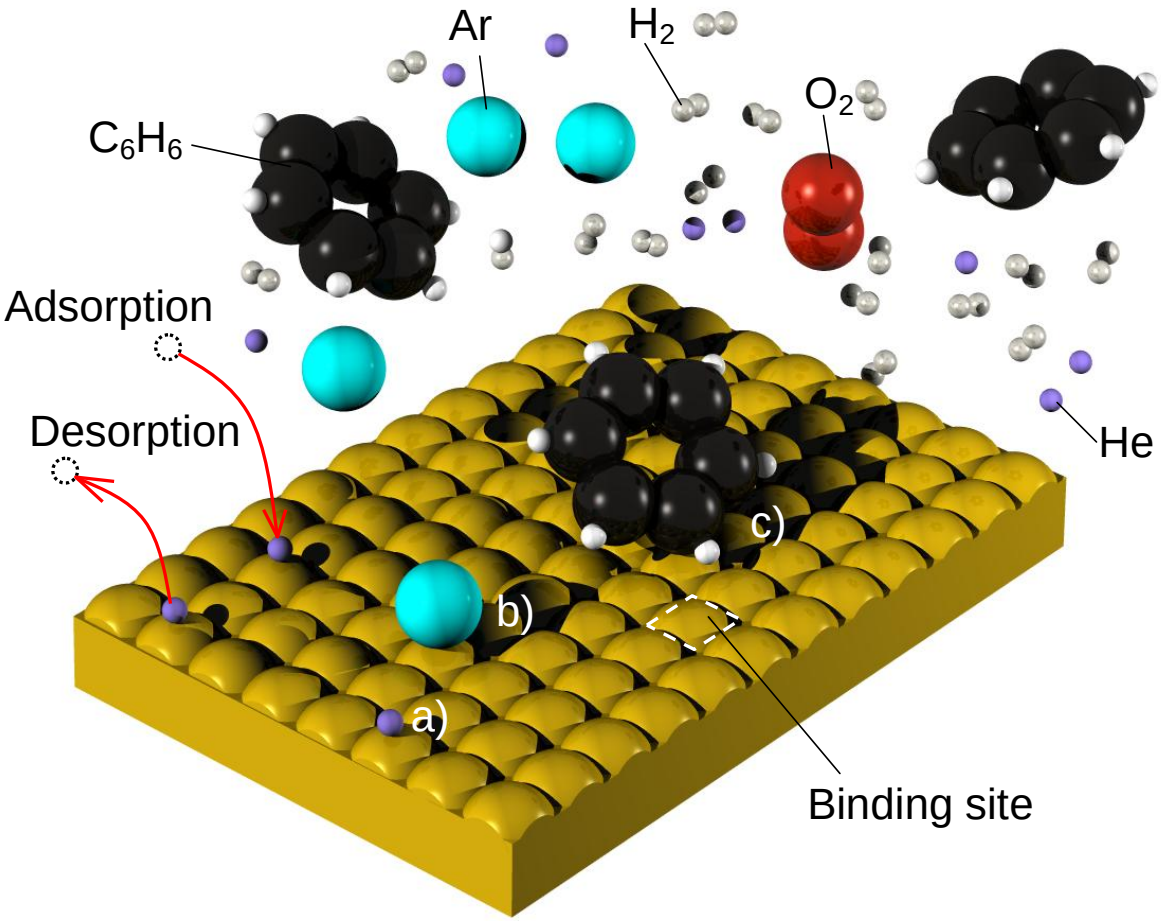

Figure 1 Schematic representation of the homogeneous surface of an adsorbent surrounded by a mixture of different gases. White dashed outline defines a single binding site. Three cases of physisorption of different species are shown: a) helium atom (monatomic gas, size smaller than the binding site dimensions); b) argon atom (here comparable to the binding site size); c) benzene molecule (much larger than the binding site)

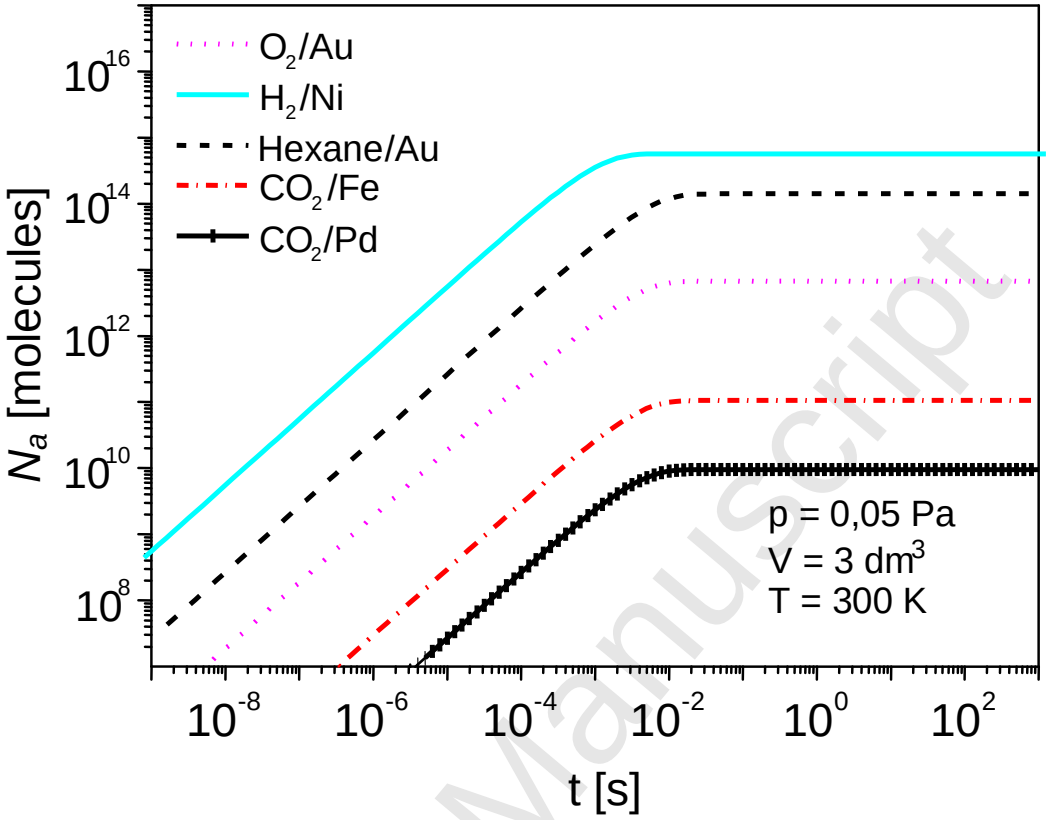

Figure 2 Time evolution of the number of adsorbed molecules in case of single-component adsorption for six different realistic situations. Black dashed line: hexane on gold, dotted magenta line: oxygen on gold, cyan solid line: hydrogen on nickel, red dash dotted line: carbon dioxide on iron; black solid line with symbol |: carbon dioxide on palladium

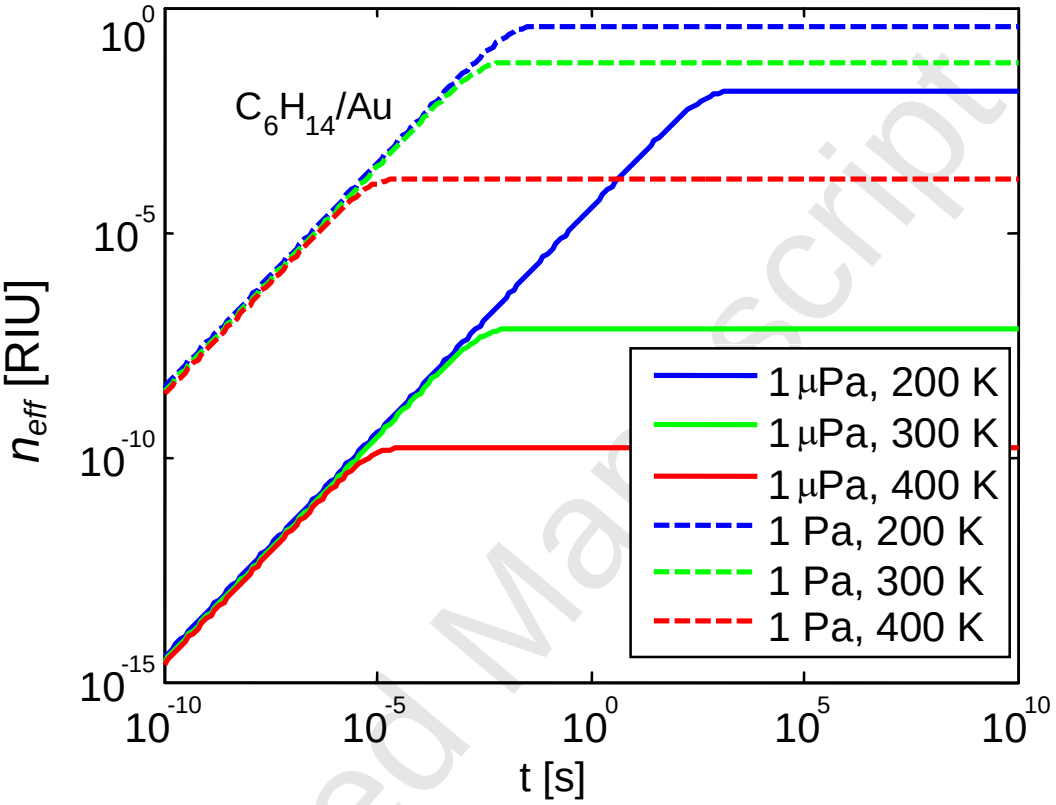

Figure 3 Time evolution of the refractive index due to hexane adsorption on gold for different pressures and temperatures. Dashed lines correspond to pressure of 1Pa and solid lines correspond to pressure of 1 μPa. Thin blue lines correspond to temperature of 200 K, thicker green lines correspond to temperature of 300 K and thickest red lines correspond to temperature of 400 K

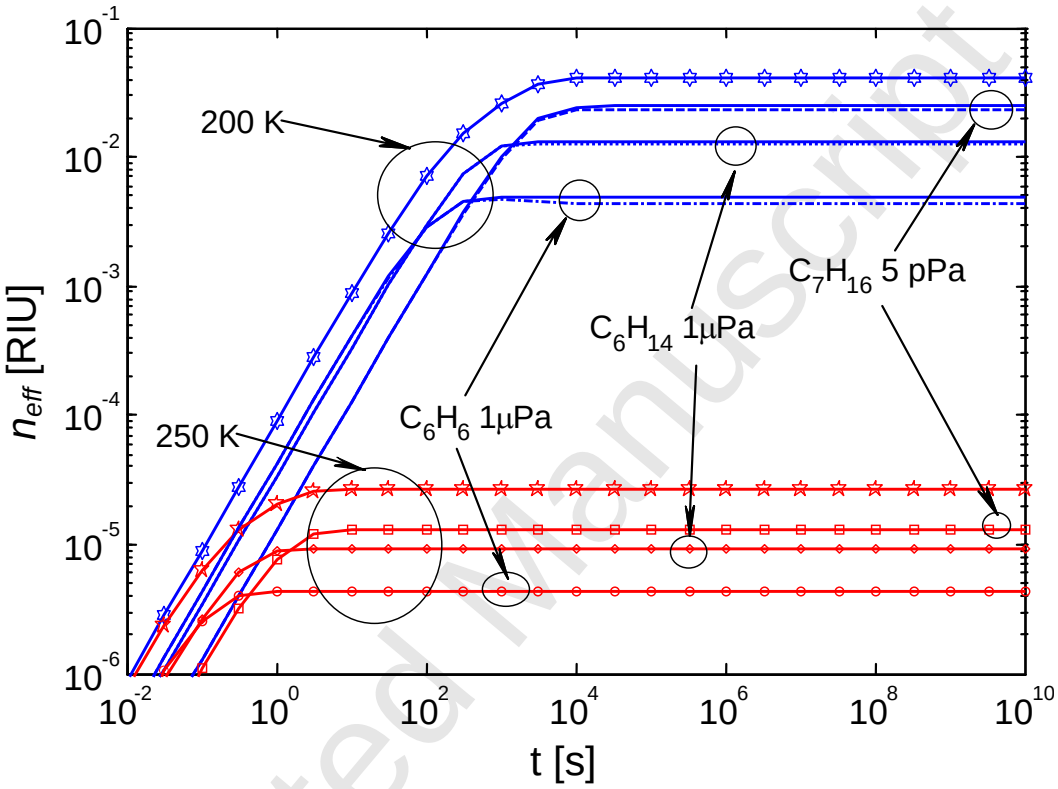

Figure 4 Time evolution of the refractive index due to adsorption of 3 gas mixture (hexane and benzene at 1 μPa, heptane at 5 pPa) on plasmonic sensor active surface of gold for different pressures and temperatures, represented with a red solid line. Dashed line corresponds to calculated component due to hexane contribution, dashed line corresponds to calculated component due to heptane contribution, and dash-dot line corresponds to calculated component due to benzene contribution. Next to each component, blue solid line corresponds to the refractive index change due to the presence of that particular gas alone on its unchanged partial pressure and at the same temperature of 200 K

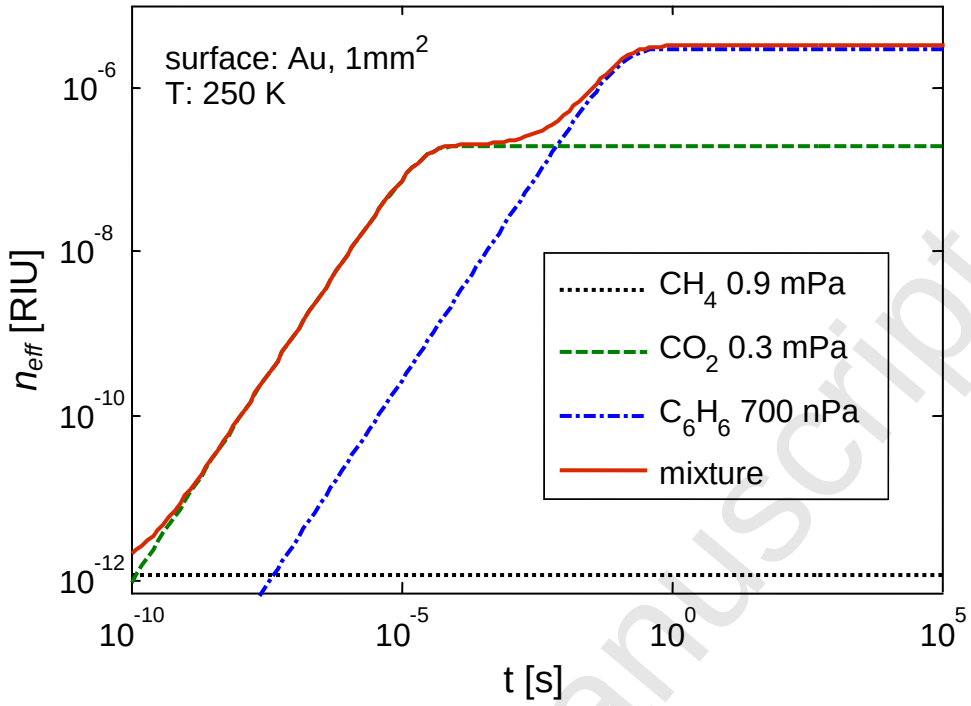

Figure 5 Time evolution of the refractive index due to adsorption of three-gas mixture (methane at partial pressure of 0.9 mPa, carbon-dioxide at partial pressure of 0.3 mPa and benzene at partial pressure of 700 nPa) on gold at a temperature of 250 K (Red solid line.) Calculated contribution of methane corresponds to dotted black line, blue dash-dot is used for benzene and green dashed for carbon-dioxide.

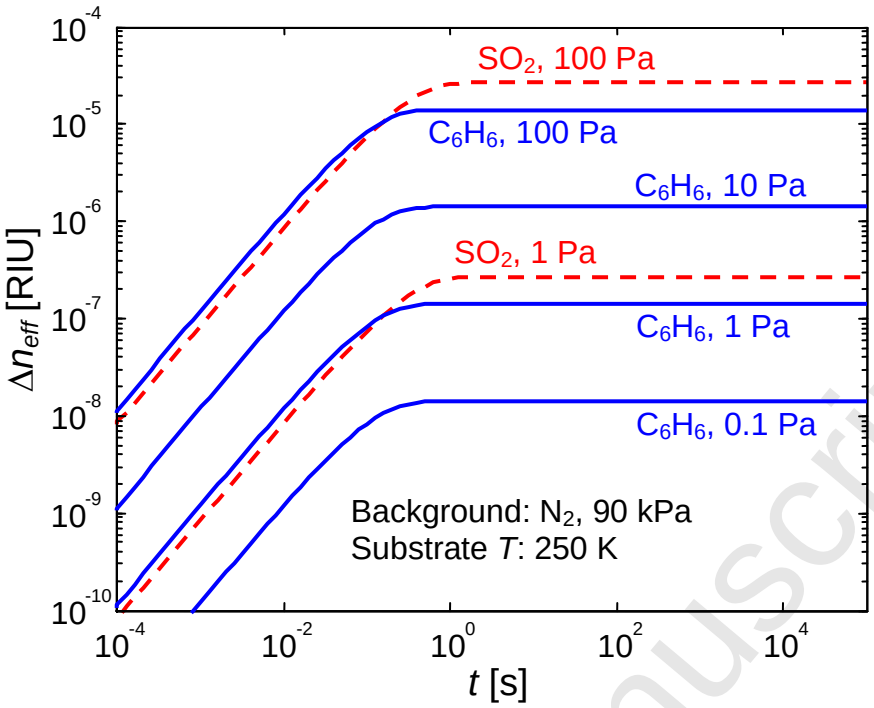

Figure 6. Time evolution of the refractive index change due to adsorption of gases in case of non-zero background. Benzene (solid lines, blue) or sulfur dioxide (dashed lines, red) are added in the initial moment $t = 0$ to a nitrogen atmosphere. N_2 partial pressure is 90 kPa, while C_6H_6 partial pressures are (0.1 – 100) Pa, and SO_2 pressures are 1 Pa and 100 Pa.

Figure

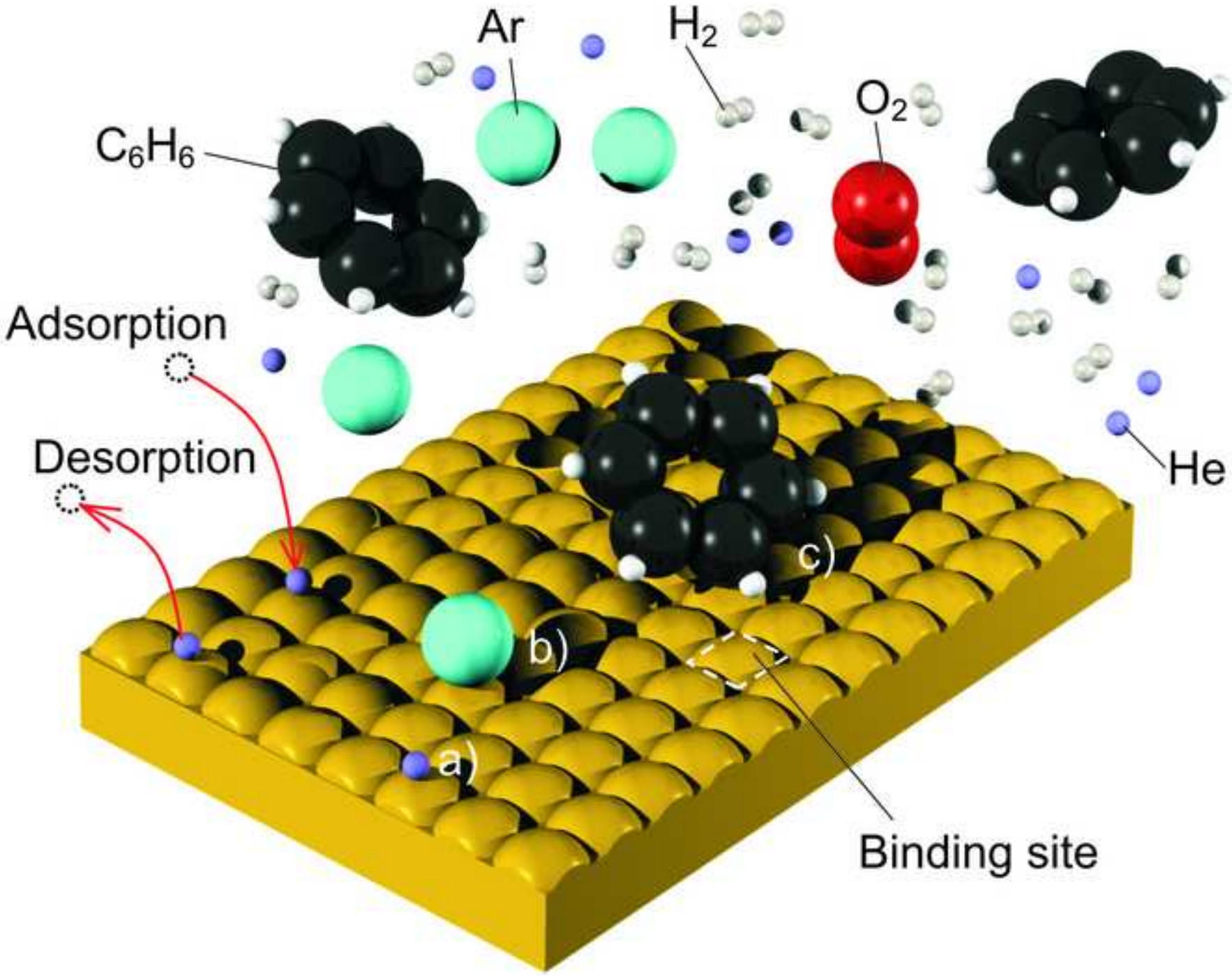

Figure

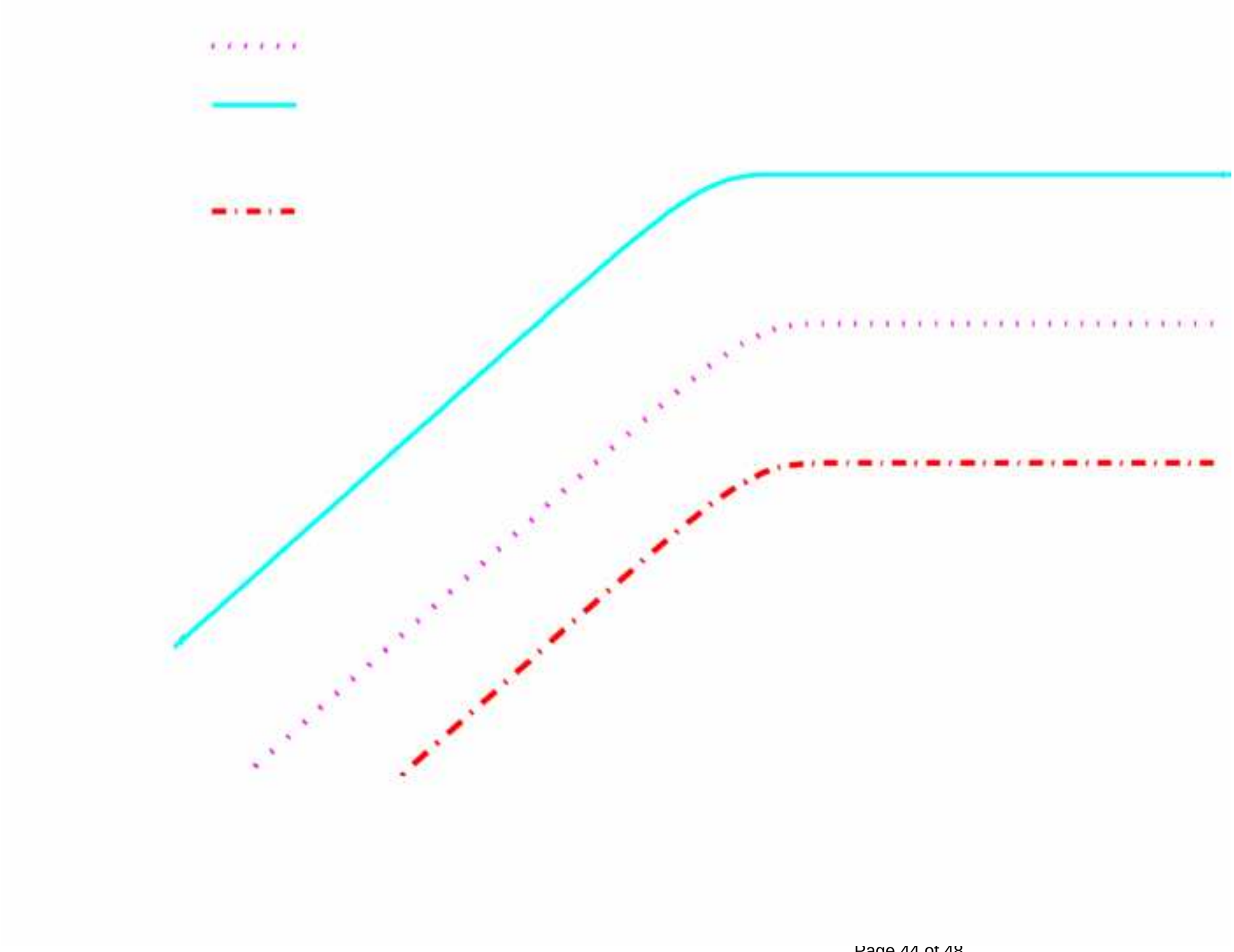

Figure

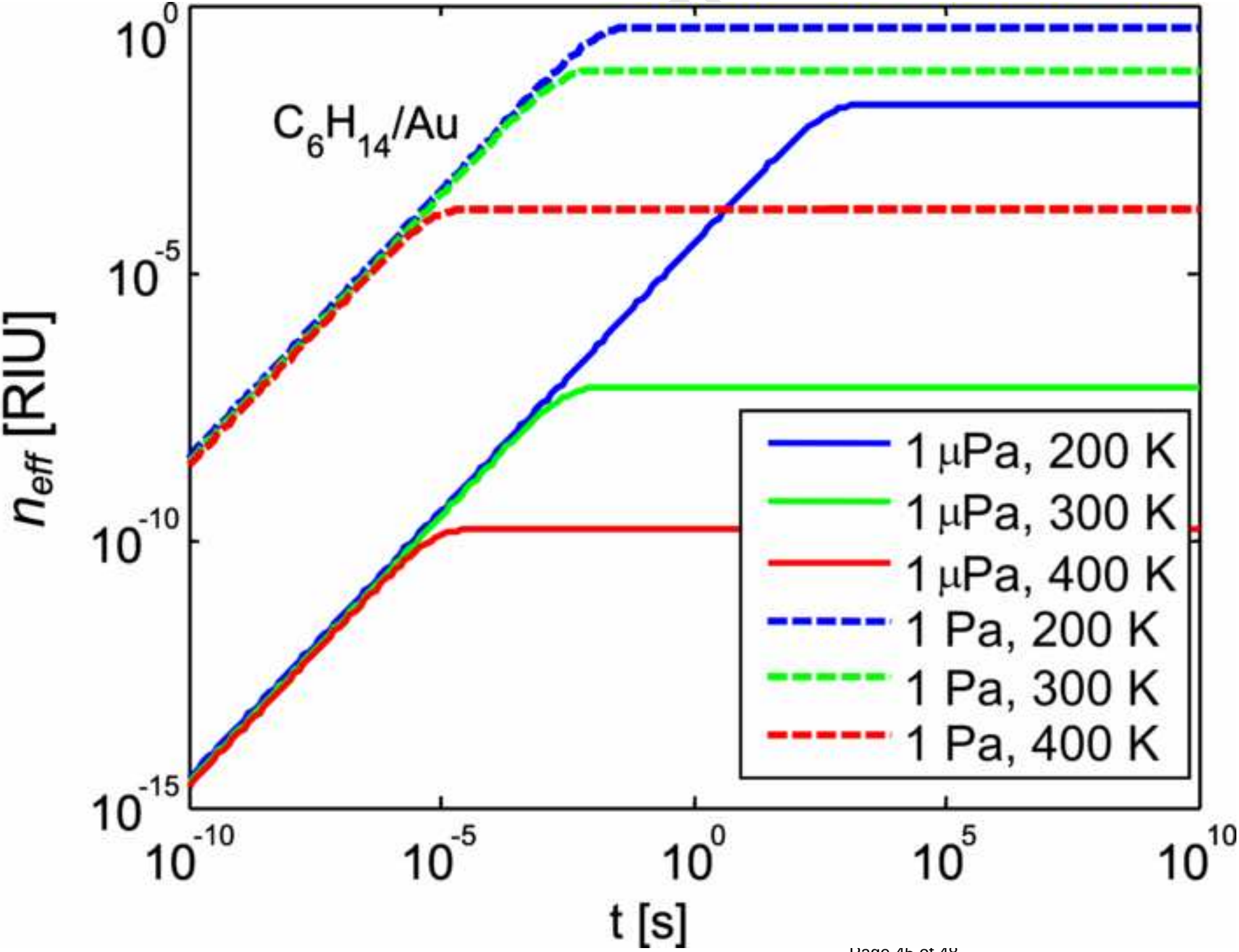
C_6H_{14}/Au
n_{eff} [RIU]
t [s]
10^{0}
10^{-5}
10^{-10}
10^{-15}
10^{-10}
10^{-5}
10^{0}
10^{5}
10^{10}
1 μPa, 200 K
1 μPa, 300 K
1 μPa, 400 K
1 Pa, 200 K
1 Pa, 300 K
1 Pa, 400 K

Figure

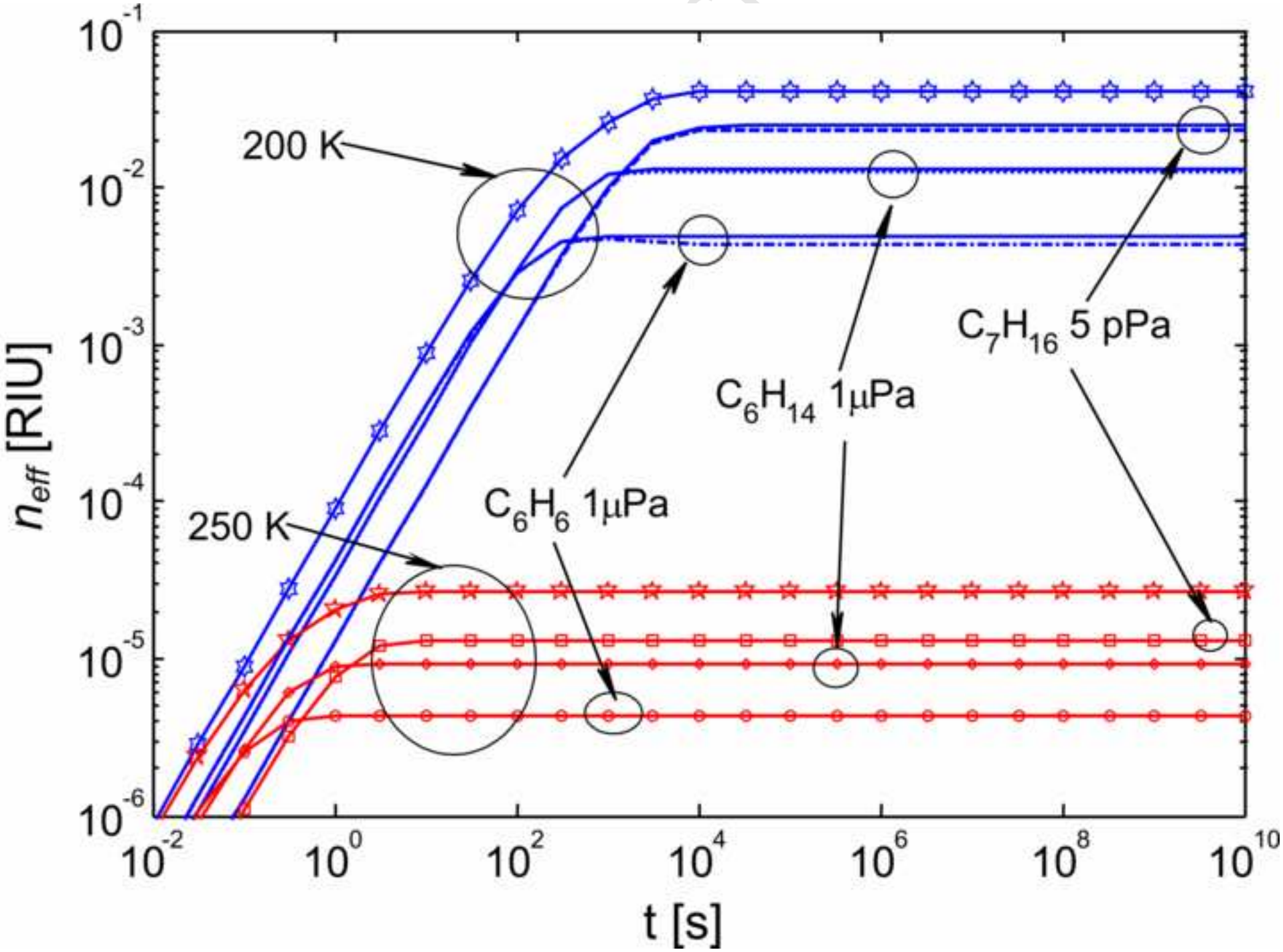
200 K
250 K
C6H6 1μPa
C6H14 1μPa
C7H16 5 pPa
neff [RIU]
t [s]
10-1
10-2
10-3
10-4
10-5
10-6
10-2
100
102
104
106
108
1010

Figure

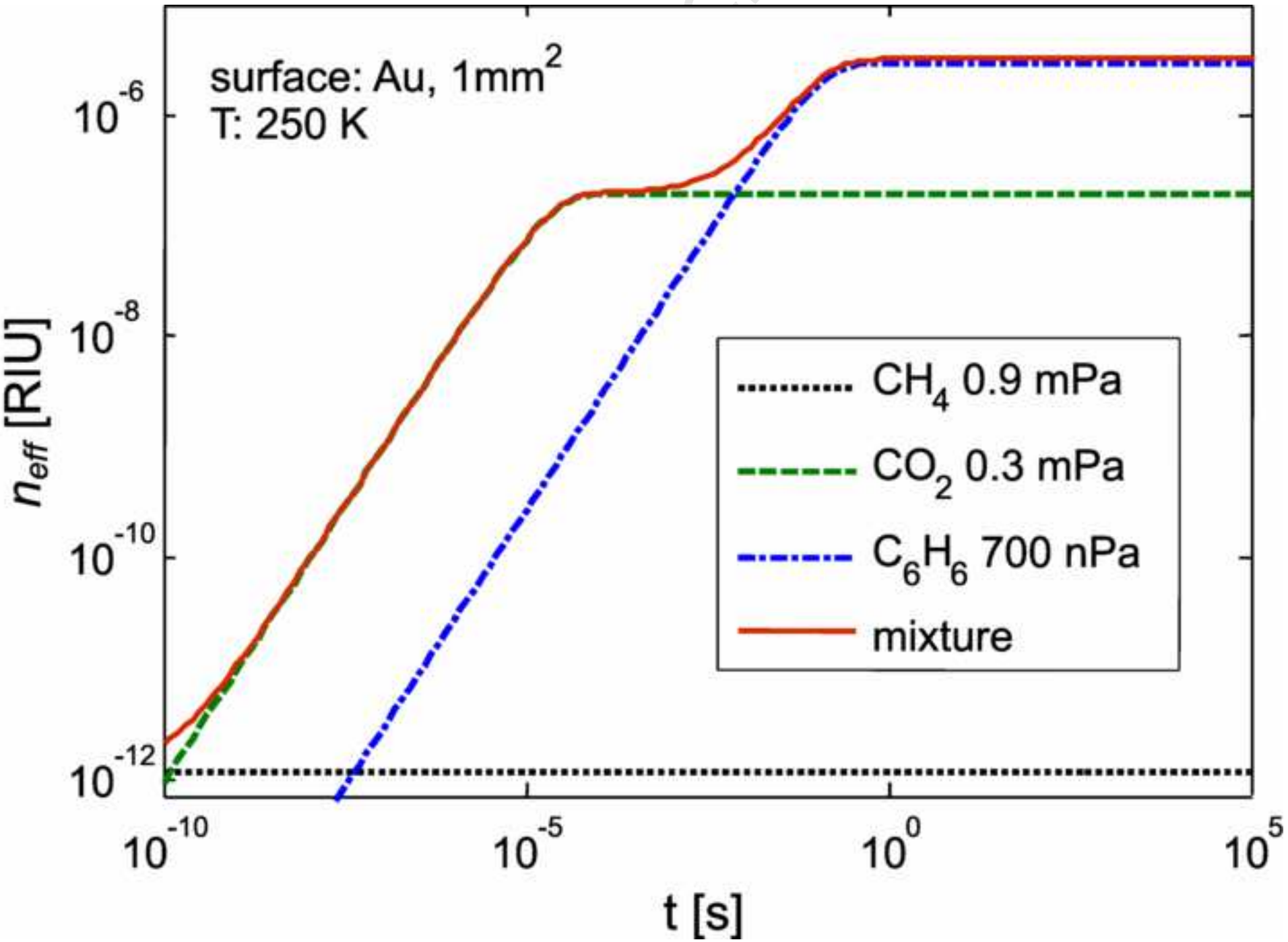
surface: Au, 1mm2
T: 250 K
CH4 0.9 mPa
CO2 0.3 mPa
C6H6 700 nPa
mixture
neff [RIU]
t [s]
10-6
10-8
10-10
10-12
10-10
10-5
100
105

Figure

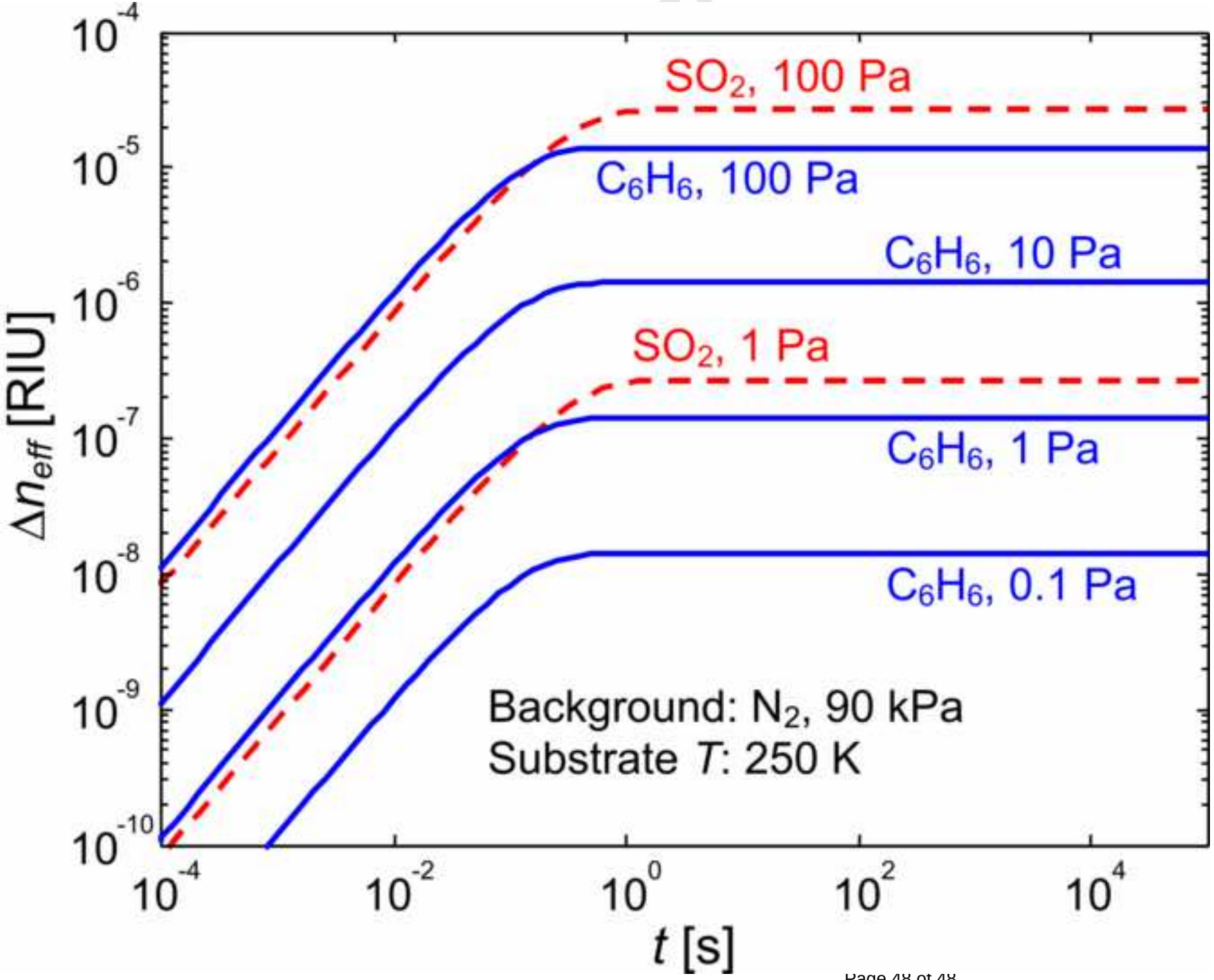
10^{-4}
10^{-5}
10^{-6}
10^{-7}
10^{-8}
10^{-9}
10^{-10}
Δn_{eff} [RIU]
SO_2, 100 Pa
C_6H_6, 100 Pa
C_6H_6, 10 Pa
SO_2, 1 Pa
C_6H_6, 1 Pa
C_6H_6, 0.1 Pa
Background: N_2, 90 kPa
Substrate T: 250 K
10^{-4}
10^{-2}
10^{0}
10^{2}
10^{4}
t [s]